Table 1
Patient demographic data

	HCC (n=11)	FNH (n=10)
SCTA acquisition	9	4
Age in years (mean)	63.8	36.2
Sex (male:female)	6:5	6:4
Underlying liver disease		
None	2	10
HBV	3	0
HCV	5	0
Alcoholic cirrhosis	1	0
Size in millimeters (mean)	45.3	27.3
Confirmation of diagnosis		
Operation	3	1
Biopsy	3	3
Clinical	5	6
Pathological diagnosis		
Well differentiated	2	
Moderately differentiated	3	
Poorly differentiated	0	
Combined	1	
FNH		4

in the liver parenchyma because of T_2 shortening [11]. In HCC, the number of Kupffer cells decrease; thus, SPIO does not accumulate in HCC, and hence, HCC shows hyperintense lesion [12]. On the other hand, the number of Kupffer cells increases in FNH [13], and as a result, SPIO accumulates in the lesion, and thus, the signal of the lesion decreases. While this is useful to distinguish FNH from other lesions [14], sometimes we encounter difficult cases because of only a slight signal decrease.

Thus, we thought that it would be useful to acquire liver lesion images reflecting the hemodynamic status in addition to SPIO-enhanced MRI. The strong susceptibility effect of SPIO enables evaluation of liver lesion vascularity using rapid injection and acquisition echo-planar sequence [15,16]. This method allows acquisition of several slices quickly and repeatedly and makes it possible to grasp the hemodynamics of liver lesions. We performed perfusion studies with SPIO and compared it to SCTA with regard to the possibility of acquiring images reflecting the hemodynamics in HCC and FNH.

2. Materials and methods

This study was performed in accordance with the Helsinki Declaration, and written informed consent was obtained from all patients.

The SPIO perfusion results in 21 patients were evaluated retrospectively. The subjects included 11 HCC (6 men and 5 women, mean age=63.8 years) cases and 10 FNH (6 men and 4 women, mean age=36.2 years) cases. SCTA was also performed in nine HCC cases and four FNH cases. Demographic data are shown in Table 1. Among the 11 HCC cases, 2 had no underlying liver disease, while 3 had hepatitis B, 5 had hepatitis C, and 1 had alcoholic cirrhosis. None of the FNH cases had an underlying liver disease. The confirmation of HCC was by operation in three cases, by percutaneous biopsy in five cases, and clinically in three cases, based on elevation of tumor marker and typical radiologic findings [1]. Pathological diagnoses were well differentiated in two cases, moderately differentiated in five cases, and combined in one case. The confirmation of FNH was by operation in one case, by percutaneous biopsy in three cases, and clinically in six cases by observation of lesion stability for a minimum of 1 year and typical radiologic findings [3–5]. A central scar was observed in three lesions. The dimension of the lesion was measured using the resected specimen or plain T_1-weighted or T_2-weighted images. The dimension of HCC was 45.3±30.3 mm and that of FNH was 27.3±3.8 mm.

2.1. Single-slice CT during arteriography

Angiography-assisted CT was performed with a 16-detector multidetector-row CT (Light Speed 16, General Electric, Milwaukee, MN). After CT during arterial portography and CT hepatic arteriography were performed, celiac arteriography, superior mesenteric arteriography, and common hepatic arteriography were performed, and then the catheter was advanced into the proper, right, or left hepatic artery. SCTA was performed with the infusion of 3 ml of contrast media (Iomeprol, Eizai, Tokyo, Japan, 350 mgI/ml) at a rate of 1 ml/s in the proper, right, or left hepatic artery using a power injector. Two slices at the center of the target lesion were chosen. Scanning began immediately before initiation of the injection of contrast media with 0.8 s per rotation. A 40-s continuous scanning technique [auto mA (max, 440 mA), 120 kVp] without table feed was used to obtain two sections with a thickness of 10 mm, a beam collimation of 20 mm, and a field of view (FOV) of 22–25 cm. The patients were instructed to hold their breath as long as possible during scanning. The images were sorted at each section and observed by both cine mode and manual mode.

2.2. SPIO perfusion study

The interval between angiography-assisted CT and MRI was less than 1 month. The MR examinations were performed with 1.5-T superconducting MR units (Avanto, Siemens, Erlangen, Germany). After T_1-weighted and T_2-weighted images were obtained, the SPIO perfusion study was performed. Bolus injectable ferucarbotran (Resovist, Bayer Schering Pharma, Osaka, Japan) was used. A total dose of 1.4 ml of ferucarbotran was used per patient. Ferucarbotran was rapidly administered at a rate of 2 ml/s by pushing with 40 ml of physiological saline using a power injector. Because the dose of ferucarbotran was very low, it could not be placed in the power injector; therefore, it was pooled in the elongation tube and pushed with physiological saline. For the perfusion study, the echo-planar method (EPI)

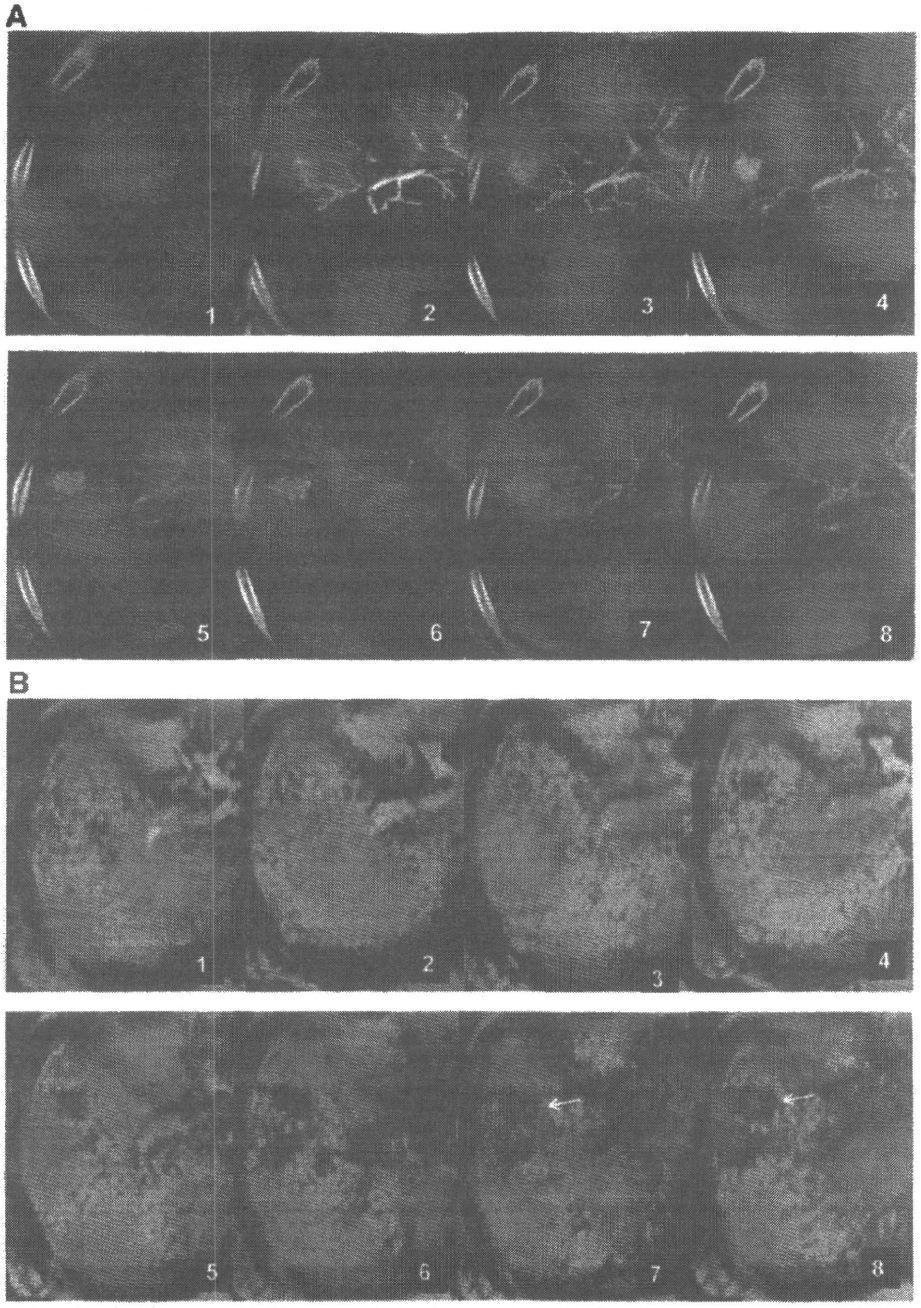

Fig. 1. A 52-year-old man with HCC. (A) SCTA. (B) SPIO perfusion study. SCTA shows centripetal enhancement in the tumor and corona enhancement (arrow). The SPIO perfusion also shows the same enhancement pattern direction and signal reduction in the area surrounding the tumor after transient signal reduction in the tumor (arrowhead). The signal reduction surrounding the tumor corresponds to corona enhancement in SCTA.

was employed. In the 12 initial patients, the scan parameters were as follows: TR, 1150 ms; TE, 20 ms; FA, 70°; EPI factor, 154; matrix, 192×154; bandwidth, 1628 Hz per pixel; FOV, 280–350 mm. Slice thickness was 7 mm. In the sequence using fat saturation and parallel imaging, the generalized autocalibrating partially parallel acquisition algorithm was utilized with an acceleration factor (iPAT factor) of 2. Imaging was obtained before administration of contrast media and 2 s after the start of administration; images were taken during a breath-hold of more than 20 s. Fifteen slice images were obtained per 1.2 s. In the latter nine patients, the scan parameters were changed to improve the time resolution; acquisition slices decreased by six slices and six slice images were obtained per 0.46 s. The scan

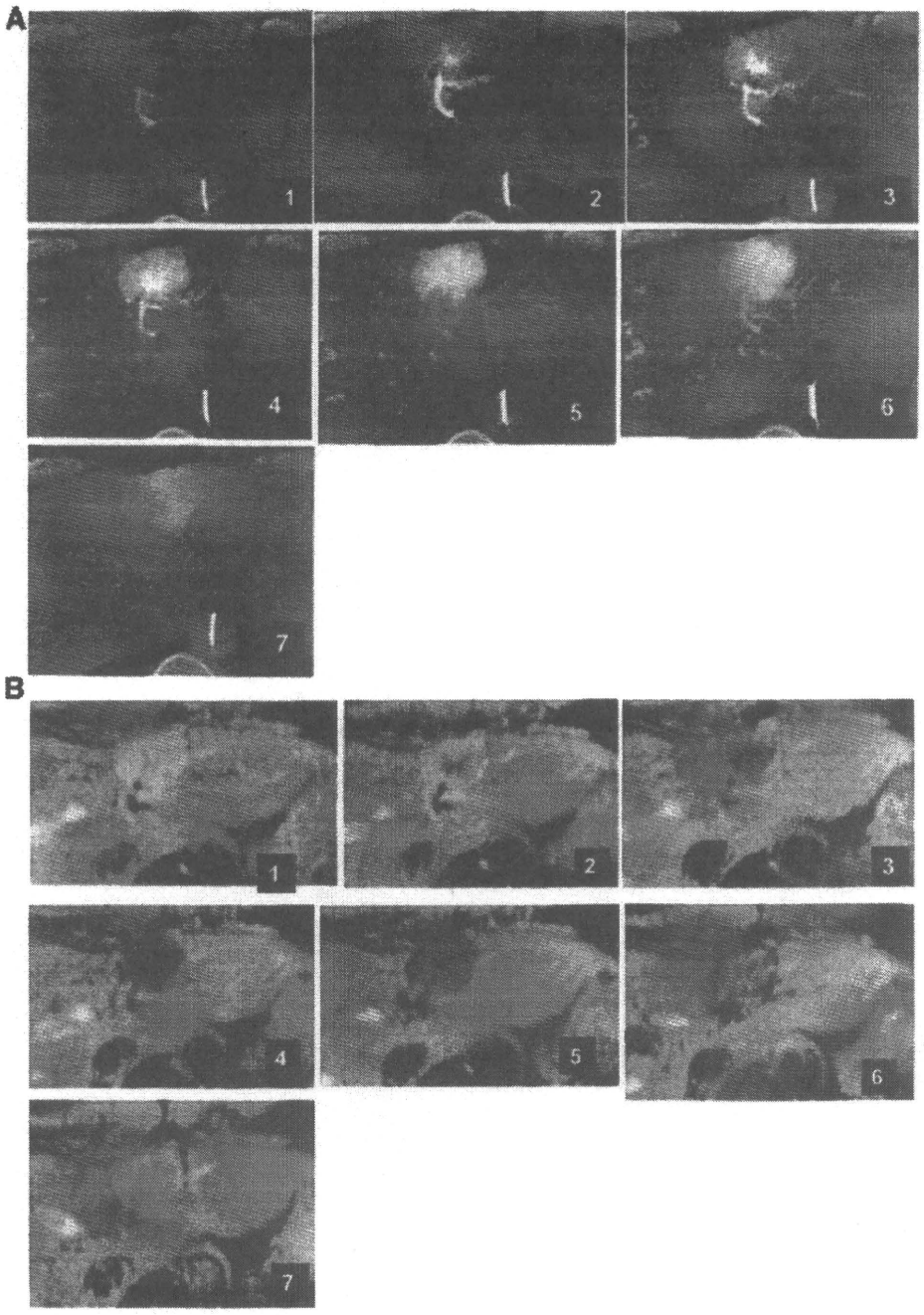

Fig. 2. A 34-year-old man with FNH. (A) SCTA. (B) SPIO perfusion study. SCTA shows centrifugal enhancement in the lesion. Fibrous septa and central scars are observed in the lesion. SPIO perfusion study also shows the same direction of the enhancement pattern. Corona enhancement is not observed by both modalities.

parameters were as follows: TR, 460 ms; TE, 20 ms; FA, 90°; matrix, 192×156. The other parameters remained unchanged. After 3 min of administration, T_1-weighted images were obtained. Ten minutes after administration, T_2-weighted fast spin-echo images and T_2^*-weighted images were taken. The images were sorted at each section and observed by both cine mode and manual mode.

2.3. Image analysis

2.3.1. SCTA versus SPIO perfusion study

SCTA was observed by two doctors whose specialty was liver imaging (16 and 6 years' experience), without patient information. The evaluation item included the vascularity of the lesion, the direction of the enhancement, and the presence

of corona enhancement. The vascularity was classified as hypervascular, isovascular, or hypovascular, in comparison to surrounding liver parenchyma. The direction of the enhancement was classified into centrifugal, centripetal, or all over the lesion simultaneously. Concerning the corona enhancement [8], it was identified as present or absent.

After evaluation of SCTA, we evaluated the SPIO perfusion study without patient information. The evaluation was performed by the same two observers after an interval of more than 2 weeks in order to prevent bias. The rapid decrease in the lesion signal corresponded to the lesion vascularity [15,16]. The evaluation of the enhancement direction in the lesion was the same as that in SCTA, classified into centrifugal, centripetal, or all over the lesion simultaneously. A decrease in the signal of the area surrounding the lesion after the transient signal decrease in the lesion, which corresponded to the corona enhancement, was observed, and any signal changes were recorded.

The two observers evaluated by consensus reading, and in case of disagreement, they had a discussion until a decision was made.

2.3.2. SPIO perfusion study

The vascularity of the lesion, the direction of the enhancement in the lesion, and the presence of the decrease in the signal of the liver parenchyma surrounding the lesion after the transient signal decrease in the lesion were evaluated (n=21 subjects, including those who only underwent SPIO perfusion).

3. Results

3.1. SCTA and SPIO perfusion study

3.1.1. Vascularity of the lesion

All 13 lesions appeared hypervascular on SCTA. All of the lesions showed a rapid decrease in lesion signal on SPIO perfusion (Fig. 1).

3.1.2. Direction of blood flow in the lesion

HCC showed centripetal enhancement in four patients, total enhancement simultaneously in three patients, and centrifugal enhancement in two patients on SCTA. The findings of SPIO perfusion almost completely agreed with the findings of SCTA.

FNH showed centrifugal enhancement in two patients, centripetal enhancement in one patient, and total enhancement simultaneously in one patient (Fig. 2). The findings of SPIO perfusion almost completely agreed with the findings of SCTA.

3.1.3. Corona enhancement

Eight of nine HCC patients showed corona enhancement in SCTA. One patient, whose exophytic lesion was confirmed to be well-differentiated HCC by resection, showed no corona enhancement. The findings of SPIO perfusion substantially agreed with the findings of SCTA (Fig. 1) except for this exophytic lesion.

FNH showed no corona enhancement on SCTA in all four patients. No decrease in the signal of the area surrounding the lesion after rapid decrease in the signal of the lesion was observed on SPIO perfusion (Fig. 2).

3.2. SPIO perfusion study

3.2.1. Vascularity of the lesion

All 21 patients showed a rapid decrease in the lesion signal.

3.2.2. Direction of blood flow in the lesion

Among 11 HCC patients, the enhancement pattern in the lesion was centripetal in 6, total enhancement simultaneously in 3, and centrifugal in 2 patients.

In the 10 FNH patients, the enhancement pattern in the lesion was centripetal in 1, total enhancement simultaneously in 1, and centrifugal in 8 patients.

3.2.3. Corona enhancement

A decrease in the signal of the liver parenchyma surrounding the lesion after the rapid decrease in the signal of the lesion was observed in 10 of 11 HCC. The only lesion in which it was not observed was the exophytic HCC.

No decrease in the signal of the liver parenchyma surrounding the lesion after the rapid decrease in the signal of the lesion was seen in any FNH case.

4. Discussion

We set out to determine whether SPIO perfusion would be effective not only as a contrast medium for FNH and HCC but also to obtain useful hemodynamics information. We supposed that it would be possible to observe the vascular structure in the lesion and of the drainage vein, as in angiography-assisted CT [9], because SPIO perfusion studies could allow repeated scanning of multislices during very short times [15,16]. The spoke-wheel appearance of centrifugal spreading vessels of the feeding artery is a well-known finding in FNH [5]. We expected to observe this finding with SPIO perfusion as well. On the other hand, it has been reported that corona enhancement indicates drainage vessels from the tumor indirectly [8] based on studies of angiography-assisted CT, and we also expected to obtain this finding by SPIO perfusion. SPIO perfusion has the advantages of being less invasive and not involving radiation exposure, in comparison to angiography-assisted CT. Moreover, we expected that SPIO perfusion could provide new additional information.

We confirmed the possibility of the evaluation of tumor vascularity as in previous studies [15,16] and also the possibility of evaluating the direction of tumor enhancement.

The evaluation of the direction of tumor enhancement with angiography-assisted CT and dynamic US under intra-arterial injection of carbon dioxide microbubbles has been reported [7,9], but these examinations could not describe multisections, which makes the description of centrifugal enhancement not necessarily easy. A spoke-wheel appearance was seen in 57–90% of FNH patients [5,6]; thus, not only was it not always possible to detect, but the possibility of false negative results had to be confirmed by multisection scanning as well. SPIO perfusion has the potential to compensate for these faults and, therefore, appears useful.

SPIO perfusion also showed the signal loss in parenchyma surrounding the tumor after transient signal loss of the tumor, which corresponded to corona enhancement in cases of HCC. On the other hand, a signal change corresponding to corona enhancement could not be seen in cases of FNH, and thus, it was possible to evaluate drainage vessels indirectly by the SPIO perfusion study. Fukukura et al. [10] reported that FNH had two drainage pathways: one pathway was venous drainage connected directly to the central or hepatic veins surrounding the lesions, while the other pathway was through the intranodular sinusoids that are connected to sinusoids in the surrounding liver. Ueda et al. [9] observed the contour of the lesion enhancement changing from an irregular shape to a round shape in the late phase of SCTA, and this finding indicated that the drainage was through the intranodular sinusoids that are connected to sinusoids in the surrounding liver. We did not encounter this type, but if the main drainage vessels are through the intranodular sinusoids to sinusoids in the surrounding liver, this might cause signal loss in the surrounding liver. Biopsy may be necessary to diagnose such cases.

In this study, CT was repeated on the same slices every 0.8 s in SCTA, and MRI was repeated on the same slices every 1.15 s in the initial 12 cases. SPIO perfusion had a disadvantage in time resolution; nevertheless, there was no difference in evaluation of the direction of the lesion enhancement. In the last nine cases, SPIO perfusion repeated scanning on the same slices every 0.46 s, and hence, the time resolution of SPIO perfusion was superior to that of SCTA. On the other hand, the spatial resolution of SPIO perfusion was inferior to that of SCTA, but it was enough to evaluate the direction of the lesion enhancement.

Gd-DTPA or SPIO has previously been used for the evaluation of perfusion in tumor [15–17]. Echo-planar sequences were used in all reports. Gd-DTPA is an extracellular contrast media, and it rapidly distributes in extravascular spaces after administration. However, SPIO presents intravascular space in the early phase and is gradually phagocytosed by reticuloendothelial cells. SPIO passes into the tumor vessels and has a transient signal loss because of its susceptibility effect; thus, the contrast medium distributing in extravascular spaces is not desirable. Therefore, contrast medium that is limited to intravascular space is advantageous to observing hemodynamics in and around the tumor. That is why we used SPIO in this study.

The limitation of this study was that we could not compare the findings of SPIO perfusion with resected specimens in detail, but we made a comparison with SCTA, a standard for diagnosis of hemodynamics in hepatic lesions, and were able to show that the findings of SPIO perfusion were comparable with those of SCTA. In this study, the subjects of HCC were overt HCC, and no hypovascular HCC cases were included. Concerning this point, we believe that it would not be difficult to distinguish hypovascular nodules from FNH.

In conclusion, SPIO perfusion is useful to evaluate the hemodynamics of hypervascular hepatocellular nodules and has the advantages of being noninvasive and not involving radiation exposure. SPIO not only is effective as a liver-specific contrast agent but also provides hemodynamics information concerning liver lesions.

References

[1] Itoh K, Nishimura K, Togashi K, Fujisawa I, Noma S, Minami S, Sagoh T, Nakano Y, Itoh H, Mori K. Hepatocellular carcinoma: MR imaging. Radiology 1987;164:21–5.
[2] Yamashita Y, Mitsuzaki K, Yi T, Ogata I, Nishiharu T, Urata J, Takahashi M. Small hepatocellular carcinoma in patients with chronic liver damage: prospective comparison of detection with dynamic MR imaging and helical CT of the whole liver. Radiology 1996;200:79–84.
[3] Mortele KJ, Praet M, Van Vlierberghe H, Kunnen M, Ros PR. CT and MR imaging finding in focal nodular hyperplasia of the liver: radiologic–pathologic correlation. AJR 2000;175:687–92.
[4] Carlson SK, Johnson CD, Bender CE, Welch TJ. CT of focal nodular hyperplasia of the liver. AJR 2000;174:705–12.
[5] Rogers JV, Mack LA, Freeny PC, Johnson ML, Sones PJ. Hepatic focal nodular hyperplasia: angiography, CT, sonography, and scintigraphy. AJR 1981;137:983–90.
[6] Mathieu D, Brunetон JN, Drouillard J, Pointreau CC, Vasile N. Hepatic adenomas and focal nodular hyperplasia: dynamic CT study. Radiology 1986;160:53–8.
[7] Kudo M, Tomita S, Tochio H, Kashida H, Hirasa M, Todo A. Hepatic focal nodular hyperplasia: specific findings at dynamic contrast-enhanced US with carbon dioxide microbubbles. Radiology 1991;179: 377–82.
[8] Miyayama S, Matsui O, Ueda K, Kifune K, Yamashiro M, Yamamoto T, Komatsu T, Kumano T. Hemodynamics of small hepatic focal nodular hyperplasia: evaluation with single-level dynamic CT during hepatic arteriography. AJR 2000;174:1567–9.
[9] Ueda K, Matsui O, Kawamori Y, Nakanuma Y, Kadoya M, Yoshikawa J, Gabata T, Nonomura A, Takashima T. Hypervascular hepatocellular carcinoma: evaluation of hemodynamic with dynamic CT during hepatic arteriography. Radiology 1998;206:161–6.
[10] Fukukura Y, Nakashima O, Kusaba A, Kage M, Kojiro M. Angioarchitecture and blood circulation in focal nodular hyperplasia of the liver. J Hepatol 1998;29:470–5.
[11] Stark DD, Weissleder R, Elizondo G, Hahn PF, Saini S, Todd LE, Wittenberg J, Ferrucci JT. Superparamagnetic iron oxide: clinical application as a contrast agent for MR imaging of the liver. Radiology 1988;168:297–301.
[12] Yamamoto H, Yamashita Y, Yoshimatsu S, Baba Y, Hatanaka Y, Murakami R, Nishiharu T, Takahashi M, Higashida Y, Moribe N. Hepatocellular carcinoma in cirrhotic livers: detection with unenhanced and iron oxide-enhanced MR imaging. Radiology 1995;195:106–12.
[13] Tanaka M, Nakashima O, Wada Y, Kage M, Kojiro M. Pathomorphological study of Kupffer cells in hepatocellular carcinoma and hyperplastic nodular lesions in the liver. Hepatology 1996;24:807–12.

[14] Precetti-Morel S, Bellin MF, Ghebontni L, Zaim S, Opolon P, Poynard T, Mathurin P, Cluzel P. Focal nodular hyperplasia of the liver on ferumoxides-enhanced MR imaging: features on conventional spin-echo, fast spin-echo and gradient-echo pulse sequences. Eur Radiol 1999;9:1535–42.

[15] Ichikawa T, Arbab AS, Araki T, Touyama K, Haradome H, Hachiya J, Yamaguchi M, Kumagai H, Aoki S. Perfusion MR imaging with a superparamagnetic iron oxide using T2-weighted and susceptibility-sensitive echoplanar sequences: evaluation of tumor vascularity in hepatocellular carcinoma. AJR 1999;173:207–13.

[16] Saito K, Shindo H, Ozuki T, Ishikawa A, Kotake F, Shimazaki Y, Abe K. Perfusion study of hypervascular hepatocellular carcinoma with SPIO. Magn Reson Med Sci 2005;4:151–8.

[17] Ichikawa T, Haradome H, Hachiya J, Nitatori T, Araki T. Characterization of hepatic lesions by perfusion-weighted MR imaging with an echoplanar sequence. AJR 1998;170:1029–34.

Original article

Effects of intermittent Pringle's manoeuvre on cirrhotic compared with normal liver

Y. Sugiyama, Y. Ishizaki, H. Imamura, H. Sugo, J. Yoshimoto and S. Kawasaki

Department of Hepatobiliary–Pancreatic Surgery, Juntendo University School of Medicine, 2-1-1 Hongo, Bunkyo-ku, Tokyo 113-8421, Japan
Correspondence to: Dr Y. Ishizaki (e-mail: ishizaki@juntendo.ac.jp)

Background: Although patients with liver cirrhosis are supposed to tolerate ischaemia–reperfusion poorly, the exact impact of intermittent inflow clamping during hepatic resection of cirrhotic compared with normal liver remains unclear.

Methods: Intermittent Pringle's manoeuvre was applied during minor hepatectomy in 172 patients with a normal liver, 59 with chronic hepatitis and 97 with liver cirrhosis. To assess hepatic injury, delta (D)-aspartate aminotransferase (AST) and D-alanine aminotransferase (ALT) (maximum level minus preoperative level) were calculated. To evaluate postoperative liver function, postoperative levels of total bilirubin, albumin and cholinesterase (ChE), and prothrombin time were measured.

Results: Significant correlations between D-AST or D-ALT and clamping time were found in each group. The regression coefficients of the regression lines for D-AST and D-ALT in patients with normal liver were significantly higher than those in patients with cirrhotic liver. Irrespective of whether clamping time was 45 min or less, or at least 60 min, D-AST and D-ALT were significantly lower in patients with cirrhosis than in those with a normal liver. Parameters of hepatic functional reserve, such as total bilirubin, prothrombin time, albumin and ChE, were impaired significantly after surgery in patients with a cirrhotic liver.

Conclusion: Patients with liver cirrhosis had a smaller increase in aminotransferase levels following portal triad clamping than those with a normal liver. However, hepatic functional reserve in those with a cirrhotic liver seemed to be affected more after intermittent inflow occlusion.

Paper accepted 1 February 2010
Published online 28 April 2010 in Wiley InterScience (www.bjs.co.uk). **DOI:** 10.1002/bjs.7039

Introduction

Cirrhosis is a major risk factor for liver surgery. Even when liver resection is restricted to patients with well preserved liver function and no portal hypertension, morbidity is still high. As recently as two decades ago, the perioperative mortality rate was reported to exceed 10 per cent when hepatic resection was performed in patients with cirrhosis, compared with less than 4 per cent for those without cirrhosis[1]. Excessive bleeding during hepatectomy and the need for blood transfusion are associated with increased postoperative morbidity as well as poorer long-term outcome in patients with primary and secondary malignancies[2–4]. The intermittent portal triad clamping technique (Pringle's manoeuvre) is effective and simple for control of blood loss from the raw surface during hepatic parenchymal transection, and has been used widely during hepatectomy[5,6].

Although hepatic inflow occlusion can also result in hepatic ischaemia–reperfusion (IR) injury, especially in patients with a cirrhotic liver[7–9], there are few convincing clinical data regarding differences in tolerance to intermittent ischaemia and reperfusion between normal and cirrhotic liver. Experimental data obtained in rats suggest that after IR injury the serum level of aminotransferase, which is widely used as a marker of liver injury, is significantly higher in animals with cirrhotic rather than normal liver[10,11]. The purpose of this study was to investigate the impact of intermittent ischaemia and reperfusion during hepatectomy in relation to the nature of the underlying liver parenchyma in humans.

Methods

Between October 2002 and March 2009, 625 patients underwent liver resection at this institution. To eliminate

operative bias (duration of operation, clamping time, number of clampings and remnant liver volume), 211 patients who had a major hepatectomy, defined as the removal of three or more Couinaud segments[12], were excluded. Thirty-two right posterior sectionectomies and eight right anterior sectionectomies were also excluded, as were 11 donor lateral segmentectomies performed using the hemivascular occlusion technique, four paediatric cases (less than 18 years of age) and 14 hepatectomies performed without the inflow occlusion technique. Seventeen patients with moderate (30–60 per cent hepatocytes with fat droplets in the resected specimen) or severe (more than 60 per cent) steatosis in the non-tumorous liver specimen were also excluded. The remaining 328 adult patients who were scheduled for elective minor hepatic resection, defined as segmentectomy or systematic subsegmentectomy, and limited resection as non-anatomical tumour removal, using the clamp crushing technique with intermittent Pringle's manoeuvre were selected for the study. Liver biopsies taken from locations distant from the tumour were reviewed retrospectively for the presence of any underlying liver disease. Liver fibrosis was quantified according to the METAVIR score[13].

Indications for liver resection

Patients with hepatocellular carcinoma (HCC), most of whom had cirrhosis, were selected for surgery according to a published flow chart based on the presence of ascites, serum total bilirubin level and indocyanine green retention rate at 15 min (ICG-R15)[14]. This decision criterion was also applied to patients without HCC whose liver function as evaluated by the ICG-R15 test was mildly impaired. In all other patients the indication for surgery was based on tumour stage, technical feasibility and remnant liver volume.

Surgical procedure

After intraoperative ultrasonography, the gallbladder was removed, if necessary, and the liver mobilized. Intermittent Pringle's manoeuvre was applied during liver transection, and consisted of cross-clamping of the hepatoduodenal ligament using a Satinsky clamp (and the aberrant left hepatic artery, if present) for 15 min, and then releasing the clamp for 5 min, until liver resection was completed. Liver transection was performed by the Péan clamp crushing method[15]. Bleeding or bile leakage points were suture ligated. Anaesthesia was maintained according to institutional routines using muscle relaxants, and the tidal volume of ventilation was reduced by 30–40 per cent of the standard volume to decrease thoracic pressure. Central venous pressure was kept below 5 cmH_2O to reduce venous haemorrhage during transection. Red blood cells were not transfused unless haematocrit fell to below 25 per cent during surgery or to less than 20 per cent on the day after operation. Total hepatic vascular exclusion was not used, and no patient had haemodilution or intraoperative or postoperative autotransfusion.

Patient data

Data were collected before, during and after surgery in a prospective computerized database, and analysed retrospectively. Demographic data included sex, age, presence of viral infection and diagnosis. The following biochemical blood variables were assessed before operation by routine laboratory techniques: haematocrit, platelet count, aspartate aminotransferase (AST), alanine aminotransferase (ALT), lactate dehydrogenase, total bilirubin, prothrombin time, albumin, cholinesterase (ChE), creatinine and ICG-R15. Intraoperative blood loss was calculated as the volume of blood collected in the aspirator and the weight of soaked gauzes. Intraoperative blood transfusion was defined as the volume of packed red cells transfused during surgery and in the immediate postoperative period.

Postoperative surveillance included clinical examinations during the hospital stay and daily laboratory tests during the first week, including AST, ALT, prothrombin time, albumin, ChE and total bilirubin level. To assess the hepatic injury response, the delta (D)-AST (maximum level minus preoperative level) and D-ALT were measured. To evaluate postoperative hepatic functional reserve, the maximum postoperative level of total bilirubin, and minimum values of prothrombin time, albumin and ChE, were assessed. Postoperative morbidity was defined according to Dindo and colleagues[16] as any perioperative complication, including biliary complications, sepsis, and pulmonary, cardiac or wound complications. Operative mortality was defined as intraoperative death and death within 30 days after hepatectomy, and in-hospital death as death during the hospital stay.

Statistical analysis

Data were expressed as mean(s.d.) or median (range). One-way ANOVA was used to compare means between groups. On detection of a significant increase by ANOVA, *post hoc* pairwise comparisons were conducted using Tukey's test. Discrete variables were included in univariable analysis using the two-tailed χ^2 test. To identify factors affecting D-AST and D-ALT, various clinical variables were evaluated

by multiple linear regression analysis. D-AST and D-ALT were defined as dependent variables, whereas underlying liver disease and cumulative clamping time were set as independent variables. Regression analysis was carried out by simple regression on cumulative clamping time to D-AST and D-ALT. Difference in correlation coefficients of the regression lines obtained from each group was determined by testing the t value. Bonferroni correction was applied for multiple comparisons. Differences at $P < 0{\cdot}050$ were considered statistically significant. Calculations were made using statistical computer software (JMP®; SAS Institute, Cary, North Carolina, USA).

Results

There were 116 women and 212 men, with a median age of 66 (range 27–80) years. According to the underlying liver disease, patients were categorized into those with a normal liver (fibrotic score 0; 172), those with chronic hepatitis (fibrotic score 1–3; 59), and those with liver cirrhosis (fibrotic score 4; 97). Hepatic resection was performed for HCC (149 patients), cholangiocellular carcinoma (7), metastatic liver tumour (121), gallbladder carcinoma (31) and other tumours (20). Patients with liver cirrhosis were older than those with a normal liver. Viral infections were more common in patients with chronic hepatitis or liver cirrhosis than in those with a normal liver. Primary liver cancer was the main indication for hepatectomy in patients with chronic hepatitis or liver cirrhosis, whereas metastatic liver cancer was common in patients with a normal liver.

The prothrombin time of patients with cirrhosis was significantly shorter than that of those with a normal liver. The ICG clearance capacity of patients with chronic hepatitis or cirrhosis was also significantly less than that of patients with a normal liver. Platelet count, and AST, ALT, albumin, ChE and total bilirubin levels differed between groups, but haematocrit, lactate dehydrogenase and creatinine levels showed no significant intergroup differences (*Table 1*).

Intraoperative results

Type of resection, duration of operation, clamping time and number of clampings were similar in the three groups, but there were significant intergroup differences in median blood loss (220 ml in patients with a normal liver, 200 ml in those with chronic hepatitis and 315 ml in patients

Table 1 Preoperative data for patients undergoing hepatectomy using intermittent Pringle's manoeuvre

	Normal liver ($n = 172$)	Chronic hepatitis ($n = 59$)	Liver cirrhosis ($n = 97$)	P†
Sex ratio (M : F)	99 : 73	47 : 12	66 : 31	0·005‡
Age (years)*	62·6(11·5)	64·3(10·2)	67·7(8·9)§	0·001
Viral infection				< 0·001‡
None	169	10	19	
Hepatitis B	3	15	16	
Hepatitis C	0	33	61	
Hepatitis B and C	0	1	1	
Diagnosis				< 0·001‡
Hepatocellular carcinoma	4	54	91	
Cholangiocellular carcinoma	2	3	2	
Metastatic liver cancer	118	0	3	
Gallbladder carcinoma	31	0	0	
Other tumour	17	2	1	
Haematocrit (%)*	39·1(4·8)	40·4(4·5)	38·7(4·8)	0·107
Platelets ($\times 10^9$/l)*	22·0(6·5)	16·1(4·8)§	12·6(6·4)§¶	< 0·001
AST (units/l)*	24(11)	34(14)§	49(24)§¶	< 0·001
ALT (units/l)*	23(16)	37(20)§	47(28)§¶	< 0·001
LDH (units/l)*	228(187)	205(77)	212(78)	0·482
Total bilirubin (mg/dl)*	0·72(0·32)	0·78(0·28)	0·85(0·30)§	0·003
Prothrombin time (%)*	93(10)	91(7)	84(10)§	< 0·001
Albumin (g/l)*	4·0(0·4)	4·1(0·4)	3·8(0·5)¶	0·014
Cholinesterase (units/l)*	1097(281)	1048(255)	796(286)§	< 0·001
Creatinine (mg/dl)*	0·7(0·2)	1·0(1·6)	0·8(0·2)	0·063
ICG-R15 (%)*	9·8(4·5)	12·7(6·4)§	18·3(8·1)§¶	< 0·001

*Values are mean(s.d.). AST, aspartate aminotransferase; ALT, alanine aminotransferase; LDH, lactate dehydrogenase; ICG-R15, indocyanine green retention rate at 15 min. †One-way ANOVA unless indicated otherwise; ‡χ^2 test. §$P < 0{\cdot}050$ *versus* normal liver, ¶$P < 0{\cdot}050$ *versus* chronic hepatitis (Tukey's test).

with liver cirrhosis; $P = 0{\cdot}001$). The number of patients requiring blood transfusion was similar in the three groups (*Table 2*).

Biochemical evaluation of hepatocyte injury

Underlying liver disease and cumulative clamping time were significantly correlated with D-AST and D-ALT (*Table 3*). Strong positive correlations between postoperative D-AST or D-ALT and cumulative clamping time were found in patients with a normal liver, and also those with underlying chronic hepatitis or a cirrhotic liver (*Figs 1* and *2*). For D-AST, the coefficient of the regression line for normal liver was significantly higher than for cirrhotic liver ($t = 18{\cdot}01$, $P < 0{\cdot}001$) and tended to be higher than that for chronic hepatitis (not significant after Bonferroni correction; $t = 2{\cdot}32$, $P = 0{\cdot}021$) (*Fig. 1*). For D-ALT, the coefficient of the regression line for normal liver was significantly higher than that for chronic hepatitis and cirrhotic liver after Bonferroni correction ($t = 16{\cdot}22$, $P < 0{\cdot}001$ and $t = 18{\cdot}53$, $P < 0{\cdot}001$ respectively) (*Fig. 2*).

D-AST and D-ALT in relation to the duration of clamping in each group are shown in *Figs 3* and *4*. In

Table 2 Operative and postoperative data

	Normal liver ($n = 172$)	Chronic hepatitis ($n = 59$)	Liver cirrhosis ($n = 97$)	P†
Type of resection				0·472‡
One segment	1	6	7	
Two segments	12	6	6	
Partial resection				
Single tumour	123	37	65	
Multiple tumours	36	10	19	
Duration of operation (min)*	292 (45–715)	285 (145–677)	305 (170–1075)	0·580
Clamping time (min)*	42 (9–163)	45 (7–170)	50 (8–172)	0·053
Clamping time ≥ 60 min	50 (29·1)	21 (36)	39 (40)	0·168‡
No. of clampings*	3 (1–11)	3 (1–12)	3 (1–11)	0·058
Intraoperative blood loss (ml)*	220 (2–1360)	200 (10–2490)	315 (30–1360)§	0·001
No. requiring blood transfusion	1 (0·6)	3 (5)	3 (3)	0·085‡
Postoperative morbidity	28 (16·3)	15 (25)	27 (28)	0·060‡
Clavien classification[16]				0·276‡
I	13	6	7	
II	12	5	17	
IIIa	2	2	3	
IIIb	0	1	0	
IV	1	0	0	
V	0	1	0	
Operative death	0 (0)	0 (0)	0 (0)	–
In-hospital death	0 (0)	1 (2)	0 (0)	0·179‡

Values in parentheses are percentages unless indicated otherwise; *values are median (range). †One-way ANOVA unless indicated otherwise; ‡χ^2 test. §$P < 0{\cdot}050$ *versus* normal liver (Tukey's test).

Table 3 Factors affecting delta-aspartate aminotransferase and delta-alanine aminotransferase

	Parameter estimate	Standard error	95% confidence interval	P*
Factors affecting D-AST				
Underlying liver disease (liver cirrhosis)	−46·84	13·68	−60·52, −33·15	< 0·001
Underlying liver disease (normal liver)	64·40	12·26	52·14, 76·66	< 0·001
Cumulative clamping time	3·29	0·28	3·29, 4·63	< 0·001
Factors affecting D-ALT				
Underlying liver disease (liver cirrhosis)	−57·52	19·62	−77·13, −37·90	< 0·001
Underlying liver disease (normal liver)	68·32	13·12	55·19, 81·44	< 0·001
Cumulative clamping time	3·41	0·30	3·10, 3·71	< 0·001

D-AST, delta-aspartate aminotransferase; D-ALT, delta-alanine aminotransferase. *Multiple linear regression analysis.

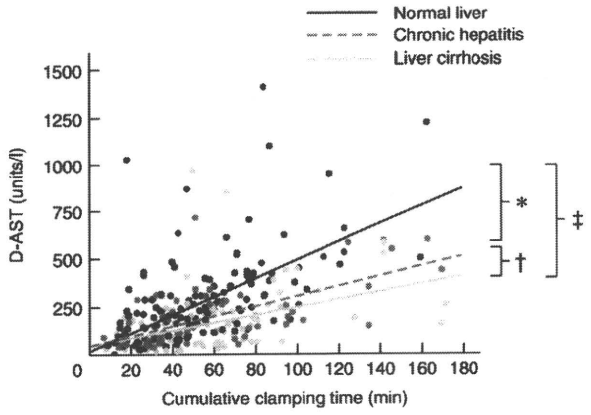

Fig. 1 Delta-aspartate aminotransferase (D-AST) level *versus* cumulative clamping time for patients with a normal liver ($y = 17{\cdot}5 + 4{\cdot}7x$; $P < 0{\cdot}001$), chronic hepatitis ($y = 47{\cdot}9 + 2{\cdot}5x$; $P < 0{\cdot}001$) or liver cirrhosis ($y = 47{\cdot}3 + 2{\cdot}0x$; $P < 0{\cdot}001$). *$P = 0{\cdot}021$, †$P = 0{\cdot}021$, ‡$P < 0{\cdot}001$ (test of t value)

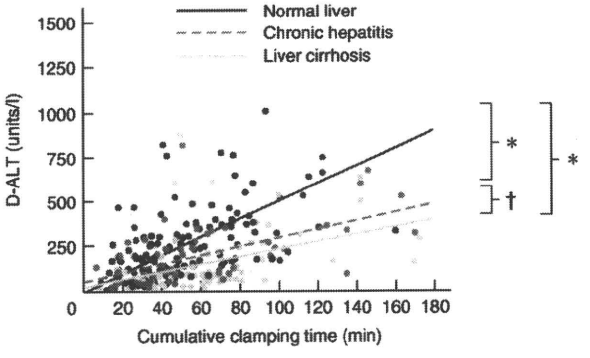

Fig. 2 Delta-alanine aminotransferase (D-ALT) level *versus* cumulative clamping time for patients with a normal liver ($y = -8{\cdot}1 + 5{\cdot}0x$; $P < 0{\cdot}001$), chronic hepatitis ($y = 52{\cdot}1 + 2{\cdot}4x$; $P < 0{\cdot}001$) or liver cirrhosis ($y = 19{\cdot}2 + 2{\cdot}1x$; $P < 0{\cdot}001$). *$P < 0{\cdot}001$, †$P = 0{\cdot}190$ (test of t value)

patients who underwent cumulative inflow occlusion for 45 min or less, D-AST and D-ALT in patients with a normal liver were significantly higher than in patients with liver cirrhosis, but did not differ significantly from those in patients with chronic hepatitis. However, in patients who underwent cumulative inflow occlusion for 60 min or longer, D-AST and D-ALT were significantly higher in patients with a normal liver than in patients with chronic hepatitis or liver cirrhosis.

Postoperative hepatic functional reserve

The postoperative maximum level of total bilirubin, and minimum values of prothrombin time, total bilirubin,

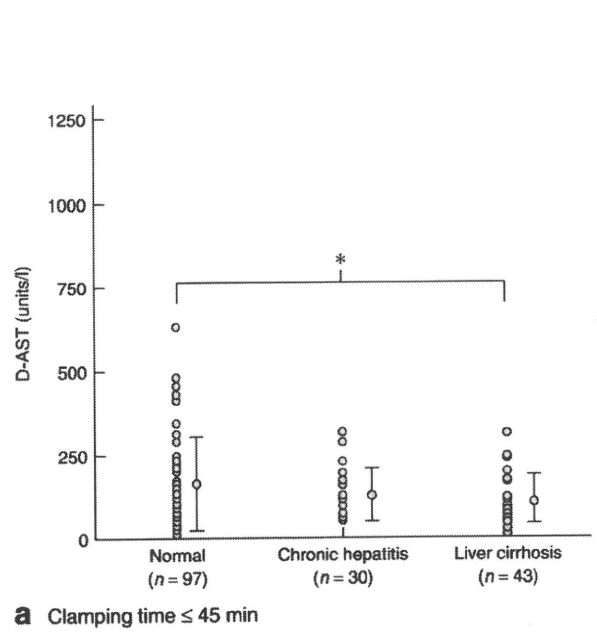

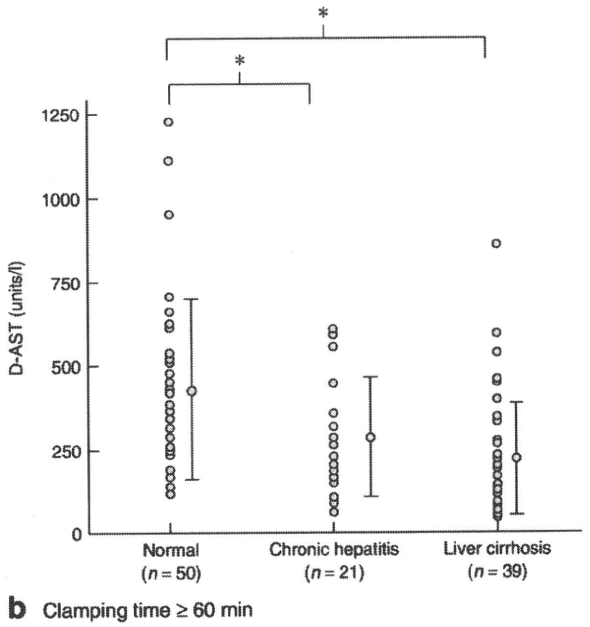

Fig. 3 Delta-aspartate aminotransferase (D-AST) level in patients with a normal liver, chronic hepatitis or liver cirrhosis with clamping time **a** 45 min or less and **b** 60 min or longer. Individual values are shown along with mean(s.d.). **a** $P = 0{\cdot}011$, **b** $P < 0{\cdot}001$ (one-way ANOVA). *$P < 0{\cdot}050$ (Tukey's test)

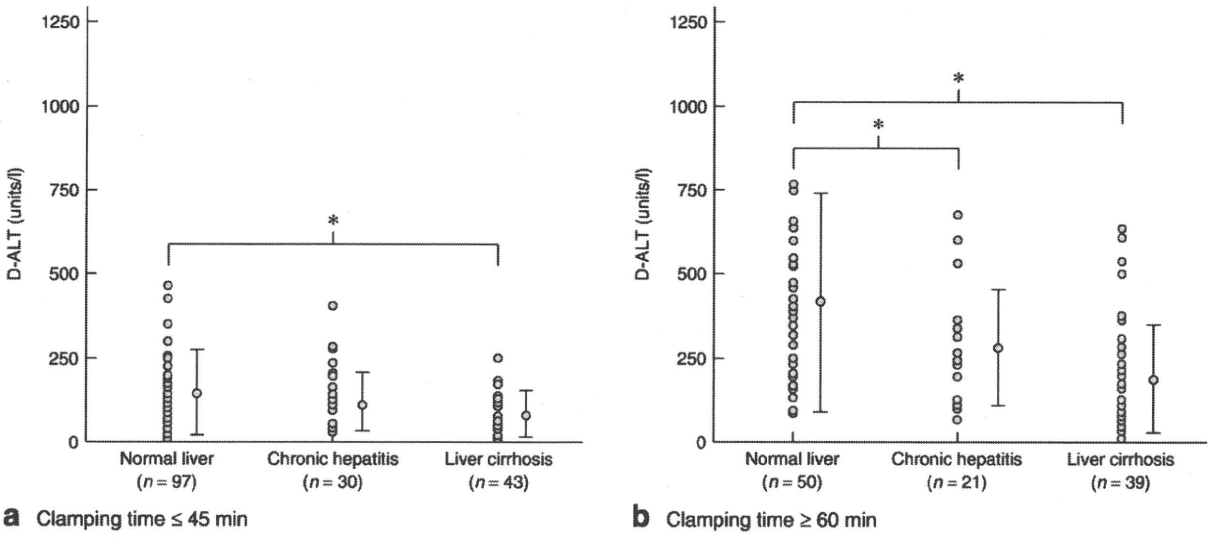

Fig. 4 Delta-alanine aminotransferase (D-ALT) level in patients with a normal liver, chronic hepatitis or liver cirrhosis with clamping time **a** 45 min or less and **b** 60 min or longer. Individual values are shown along with mean(s.d.). **a** $P = 0{\cdot}018$, **b** $P < 0{\cdot}001$ (one-way ANOVA). *$P < 0{\cdot}050$ (Tukey's test)

Table 4 Assessment of postoperative liver function

	Normal liver ($n = 172$)	Chronic hepatitis ($n = 59$)	Liver cirrhosis ($n = 97$)	P*
Maximum total bilirubin level (mg/dl)	1·25(0·58)	1·47(0·48)	1·52(0·55)†	< 0·001
Minimum prothrombin time (%)	74(13)	71(13)	68(10)†	< 0·001
Minimum albumin level (g/dl)	4·0(0·4)	4·1(0·4)	3·8(0·5)†‡	< 0·001
Minimum cholinesterase level (units/l)	558(239)	509(249)	357(179)†	< 0·001

Values are mean(s.d.). *One-way ANOVA. †$P < 0{\cdot}050$ *versus* normal liver, ‡$P < 0{\cdot}050$ *versus* chronic hepatitis (Tukey's test).

albumin and ChE, differed significantly between the three groups. Postoperative hepatic functional reserve was much more compromised in patients with a cirrhotic liver after hepatic resection (*Table 4*).

Postoperative results

The incidence and severity of postoperative complications did not differ significantly between the three groups (*Table 2*). Although there was no operative mortality, one patient with chronic hepatitis died from severe interstitial pneumonia 4 months after minor hepatectomy.

Discussion

The tolerance of cirrhotic liver to normothermic intermittent inflow occlusion is still unknown. Most investigators believe that normothermic liver ischaemia is more dangerous in cirrhotic than normal liver[17,18]. The severity of IR injury is best assessed by serial determination of serum AST or ALT levels, which are generally considered to be reliable markers of hepatocyte injury[19]. This is the first reported study to demonstrate that, in terms of aminotransferase levels, the response of AST and ALT to intermittent ischaemia differs between normal and cirrhotic liver in humans. The marked outflow of intracellular enzymes that occurred after intermittent hepatic occlusion in patients with a normal liver was less pronounced in patients with a cirrhotic liver. Isozaki and colleagues[20] examined the degree of liver injury in the remnant liver in normal and cirrhotic rats undergoing 70 per cent hepatectomy with hepatic inflow occlusion. They concluded that cirrhotic liver showed a less pronounced necrotic response to ischaemia than normal liver, as the serum AST level increased with hepatic vascular occlusion to a greater degree in rats with a normal liver than in those with a cirrhotic liver.

On the other hand, in a biochemical investigation of effects of IR in rats with experimentally induced liver cirrhosis, Nishimura and co-workers[10] showed that, at 24 h after a 30-min interruption of blood flow, the AST levels rose significantly higher in rats with liver cirrhosis than those with a normal liver. They concluded that cirrhotic livers subjected to ischaemia might have more necrotic cells than normal liver. Jang *et al.*[11] also investigated the effect of IR and showed that serum AST and ALT levels after 60 min ischaemia were significantly higher in mice with a cirrhotic liver than in those with a normal liver. Apoptosis was more evident in normal livers, whereas necrosis was a predominant feature in the cirrhotic livers[11]. These experimental studies showed that the degree of hepatic injury after IR was significantly greater in cirrhotic liver than in normal liver.

Postoperative AST and ALT levels may be related to the volume of liver resection. Clavien and colleagues[21] reported that, for matched patients with the same ischaemia time, patients with extended liver resections had lower postoperative peak AST levels than patients with smaller resection volumes. Smaller remnant liver masses might have been associated with lower postreperfusion serum AST and ALT levels than larger residual liver volumes. In the present series, to eliminate such bias created by differences in magnitude of resection or volume of liver remaining, major hepatectomies were excluded from this study. The three groups were comparable with respect to extent of liver resection and procedure. The present findings support the contention that cirrhotic liver releases smaller amounts of aminotransferase than normal liver after IR.

The results of this study do not seem to match those from randomized controlled trials[5,22] and a meta-analysis[23] of hepatic inflow clamping, which showed that chronically diseased livers are more susceptible to IR injury than normal liver. The paradoxical finding that cirrhotic liver released less aminotransferase than normal liver after IR may be unrelated to postoperative liver dysfunction. Cirrhosis is a diffuse process characterized by fibrosis and conversion of the normal liver architecture to structurally abnormal nodules. A decrease in the ratio of parenchyma to non-parenchyma in cirrhotic liver has been described[24,25]. The results of the present study may be explained by the fact that cirrhotic liver probably has fewer healthy hepatocytes per unit area than normal liver. Another drawback of hepatic clamping can be splanchnic venous stasis. It has also been suggested that the presence of collateral circulation and the absence of portal congestion in patients with a cirrhotic liver might explain the apparently better tolerance to portal cross-clamping.

Although the patients with liver cirrhosis had lower aminotransferase levels after intermittent inflow occlusion, enzymes such as AST and ALT may not be telling the whole story, and the relatively minor postoperative increase in levels, such as between 200 and 500 units/l, may have no clinical significance. More sensitive makers of liver damage, such as liver fatty acid binding protein[26–28], may shed new light on this matter. Furthermore, postoperative liver functional reserve, as indicated by values of total bilirubin, prothrombin time, albumin and ChE, was impaired significantly in patients with a cirrhotic liver.

Further studies should ideally include a more detailed assessment of liver function, as attempted previously by Schindl and colleagues[29] and Yigitler and co-workers[30]. Care should still be taken when resecting cirrhotic liver under intermittent inflow occlusion to reduce the risk of postoperative morbidity.

Acknowledgements

The authors declare no conflict of interest.

References

1 Song TJ, Ip EW, Fong Y. Hepatocellular carcinoma: current surgical management. *Gastroenterology* 2004; **127**(Suppl 1): S248–S260.
2 Laurent C, Sa Cunha A, Couderc P, Rullier E, Saric J. Influence of postoperative morbidity on long-term survival following liver resection for colorectal metastases. *Br J Surg* 2003; **90**: 1131–1136.
3 Liu CL, Fan ST, Cheung ST, Lo CM, Ng IO, Wong J. Anterior approach *versus* conventional approach right hepatic resection for large hepatocellular carcinoma: a prospective randomized controlled study. *Ann Surg* 2006; **244**: 194–203.
4 Kooby DA, Stockman J, Ben-Porat L, Gonen M, Jarnagin WR, Dematteo RP *et al.* Influence of transfusions on perioperative and long-term outcome in patients following hepatic resection for colorectal metastases. *Ann Surg* 2003; **237**: 860–869.
5 Belghiti J, Noun R, Malafosse R, Jagot P, Sauvanet A, Pierangeli F *et al.* Continuous *versus* intermittent portal triad clamping for liver resection: a controlled study. *Ann Surg* 1999; **229**: 369–375.
6 Ishizaki Y, Yoshimoto J, Miwa K, Sugo H, Kawasaki S. Safety of prolonged intermittent Pringle maneuver during hepatic resection. *Arch Surg* 2006; **141**: 649–653.
7 Kim YI, Nakashima K, Tada I, Kawano K, Kobayashi M. Prolonged normothermic ischaemia of human cirrhotic liver during hepatectomy: a preliminary report. *Br J Surg* 1993; **80**: 1366–1570.
8 Fan ST, Lai EC, Lo CM, Ng IO, Wong J. Hospital mortality of major hepatectomy for hepatocellular carcinoma associated with cirrhosis. *Arch Surg* 1995; **130**: 198–203.

9 Wu CC, Hwang CR, Liu TJ, P'eng FK. Effects and limitations of prolonged intermittent ischaemia for hepatic resection of the cirrhotic patients. *Br J Surg* 1996; **83**: 121–124.

10 Nishimura T, Nakahara M, Kobayashi S, Hatta I, Yamawaki S, Marui Y. Ischemic injury in cirrhotic livers: an experimental study of the temporary arrest of hepatic circulation. *J Surg Res* 1992; **53**: 227–233.

11 Jang JH, Moritz W, Graf R, Clavien PA. Preconditioning with death ligands fasL and TNF-α protects the cirrhotic mouse liver against ischaemic injury. *Gut* 2008; **57**: 492–499.

12 Strasberg SM. Nomenclature of hepatic anatomy and resections: a review of the Brisbane 2000 system. *J Hepatobiliary Pancreas Surg* 2005; **12**: 351–355.

13 Bedossa P, Poynard T. An algorithm for the grading of activity in chronic hepatitis C. The METAVIR Cooperative Study Group. *Hepatology* 1996; **24**: 289–293.

14 Makuuchi M, Kosuge T, Takayama T, Yamazaki S, Kakazu T, Miyagawa S. Surgery for small liver cancers. *Semin Surg Oncol* 1993; **9**: 298–304.

15 Ishizaki Y, Yoshimoto J, Sugo H, Miwa K, Kawasaki S. Hepatectomy using traditional Péan clamp-crushing technique under intermittent Pringle maneuver. *Am J Surg* 2008; **196**: 353–357.

16 Dindo D, Demartines N, Clavien PA. Classification of surgical complications: a new proposal with evaluation in a cohort of 6336 patients and results of a survey. *Ann Surg* 2004; **240**: 205–213.

17 Nagasue N, Uchida M, Kubota H, Hayashi T, Kohno H, Nakamura T. Cirrhotic livers can tolerate 30 minutes ischaemia at normal environmental temperature. *Eur J Surg* 1995; **161**: 181–186.

18 Man K, Fan ST, Ng IO, Lo CM, Liu CL, Wong J. Prospective evaluation of Pringle maneuver in hepatectomy for liver tumors by a randomized study. *Ann Surg* 1997; **226**: 704–711; discussion 711–713.

19 Nishimura T, Yoshida Y, Watanabe F, Koseki M, Nishida T, Tagawa K *et al.* Blood level of mitochondrial aspartate aminotransferase as an indicator of the extent of ischemic necrosis of the rat liver. *Hepatology* 1986; **6**: 701–707.

20 Isozaki H, Okajima K, Kobayashi M, Hara H, Akimoto H. Experimental study of liver injury after partial hepatectomy with intermittent or continuous hepatic vascular occlusion. Differences in tolerance to ischemia between normal and cirrhotic livers. *Eur Surg Res* 1995; **27**: 313–322.

21 Clavien PA, Selzner M, Rudiger HA, Graf R, Kadry Z, Rousson V *et al.* A prospective randomized study in 100 consecutive patients undergoing major liver resection with *versus* without ischemic preconditioning. *Ann Surg* 2003; **238**: 843–850; discussion 851–852.

22 Capussotti L, Nuzzo G, Polastri R, Giuliante F, Muratore A, Giovannini I. Continuous *versus* intermittent portal triad clamping during hepatectomy in cirrhosis. Results of a prospective, randomized clinical trial. *Hepatogastroenterology* 2003; **50**: 1073–1077.

23 Rahbari NN, Wente MN, Schemmer P, Diener MK, Hoffmann K, Motschall E *et al.* Systematic review and meta-analysis of the effect of portal triad clamping on outcome after hepatic resection. *Br J Surg* 2008; **95**: 424–432.

24 Ludwig J, Elveback LR. Parenchyma weight change in hepatic cirrhosis. A morphometric study and discussion of the method. *Lab Invest* 1972; **26**: 338–343.

25 Imamura H, Kawasaki S, Shiga J, Bandai Y, Sanjo K, Idezuki Y. Quantitative evaluation of parenchymal liver cell volume and total hepatocyte number in cirrhotic patients. *Hepatology* 1991; **14**: 448–453.

26 van de Poll MC, Derikx JP, Buurman WA, Peters WH, Roelofs HM, Wigmore SJ *et al.* Liver manipulation causes hepatocyte injury and precedes systemic inflammation in patients undergoing liver resection. *World J Surg* 2007; **31**: 2033–2038.

27 Hanssen SJ, Derikx JP, Vermeulen Windsant IC, Heijmans JH, Koeppel TA, Schurink GW *et al.* Visceral injury and systemic inflammation in patients undergoing extracorporeal circulation during aortic surgery. *Ann Surg* 2008; **248**: 117–125.

28 Derikx JP, Poeze M, van Bijnen AA, Buurman WA, Heineman E. Evidence for intestinal and liver epithelial cell injury in the early phase of sepsis. *Shock* 2007; **28**: 544–548.

29 Schindl MJ, Redhead DN, Fearon KC, Garden OJ, Wigmore SJ; Edinburgh Liver Surgery and Transplantation Experimental Research Group (eLISTER). The value of residual liver volume as a predictor of hepatic dysfunction and infection after major liver resection. *Gut* 2005; **54**: 289–296.

30 Yigitler C, Farges O, Kianmanesh R, Regimbeau JM, Abdalla EK, Belghiti J. The small remnant liver after major liver resection: how common and how relevant? *Liver Transpl* 2003; **9**(Suppl 1): S18–S25.

Liver / Other

SE-083

Hepatic venous phase of the liver is already affected by hepatobiliary uptake of Gd-EOB-DTPA: comparison between Gd-EOB-DTPA and Gd-DTPA in dynamic MRI on 3.0-T apparatus

Y. Fujinaga, M. Kadoya, K. Ueda, M. Kurozumi, T. Matsushita, A. Ohya, Y. Kitou, H. Ueda; Matsumoto/JP

Purpose: To reveal the difference in contrast enhancement of the liver in comparison to other abdominal structures on dynamic contrast-enhanced MRI (DCE-MRI) using gadoxetic acid (Gd-EOB-DTPA: EOB) and gadobutrol acid (Gd-DTPA) in the same patients.

Material and Methods: DCE-MRI on a 3.0-T apparatus using EOB and Gd-DTPA was performed in the same 17 patients. Precontrast and DCE-MRI images [arterial phase (AP), portal venous phase (PP), hepatic venous phase (HP)] were acquired before and after bolus injection of each contrast agent. Signal intensity ratio of organ-to-muscle [liver (L/M), spleen (S/M), aorta (A/M), portal vein (P/M) and hepatic vein (H/M)] were calculated at each phase and statistically analyzed.

Results: Between EOB and Gd-DTPA, there were no significant differences in the means of L/M, S/M, A/M, P/M or H/M on precontrast images, L/M at AP, or L/M at PP. At all phases, the mean S/M (AP, 2.06, 2.70, $p<0.01$; PP, 1.97, 2.33, $p<0.001$; HP, 1.80, 2.09, $p<0.01$), A/M (AP, 2.78, 3.50, $p<0.01$; PP, 2.36, 2.82, $p<0.001$; HP, 2.15, 2.61, $p<0.001$), P/M (AP, 1.98, 2.47, $p<0.01$; PP, 2.65, 2.96, $p<0.05$; HP, 2.30, 2.65, $p<0.01$) and V/M (AP, 1.11, 1.23, $p<0.05$; PP, 2.65, 2.84, $p<0.001$; HP, 2.22, 2.67, $p<0.001$) with EOB were all lower than the respective values with Gd-DTPA. On HP, the mean L/M (1.99, 1.88, $p<0.05$) with EOB was higher than that with Gd-DTPA.

Conclusion: On DCE-MRI on 3.0-T using EOB, contrast enhancement of all organs except for the liver was lower than that of other organs on DCE-MRI using Gd-DTPA, but that of the liver at HP was already affected by the hepatobiliary uptake of EOB.

Mesentery and Peritoneum

SE-084

Spontaneous hemoperitoneum: a diagnostic challenge

A. Karatzas, P. Kraniotis, P. Zabakis, I. Tsota, M. Tsimara, E. Konstantatou, T. Petsas, C. Kalogeropoulou; Patras/GR

Purpose: Spontaneous hemoperitoneum is an emergency condition, the diagnosis of which is usually difficult to be made only by clinical criteria.

Material and Methods: A review of our institution cases, for the last 5 years, was carried out. Examinations were performed in a 16x MDCT before and after IV contrast administration and scans were taken at arterial, portal venous and delayed phase. The presence of active bleeding and the cause of the bleeding were assessed.

Results: Ten cases of spontaneous hemoperitoneum were found. Active extravasation was present in 5 patients. In 9 cases, there were direct (active bleeding) or indirect (sentinel clot) signs that implicated the exact cause of the bleeding. In 3 circumstances, the origin of the bleeding was the liver (2 HCCs, 1 metastases from choriocarcinoma), in 2 a ruptured ovary cyst, in 1 spontaneous bleeding of the spleen, in 1 the splenic artery which had been eroded because of pancreatitis, in 1 the small intestine and in 1 cirrhotic patient a dilated portosystemic shunt. In 1 patient, the cause of bleeding was not determined initially, although sentinel clots were present in the epigastrium. Three days later, a second CT revealed an abnormal vessel at the greater curvature of the stomach, which was considered the cause of bleeding.

Conclusion: CT is the examination of choice in the diagnosis of spontaneous hemoperitoneum. In the majority of cases, it can reliably determine the cause of the bleeding.

Other / Acute and Post-Traumatic Abdomen

SE-085

Focused assessment with sonography for trauma as screening method in trauma patients with blunt abdominal injuries: a prospective study

S. Loti, I. Liovarou, S. Drossos, M. Kosmidou, A. Kopanoudis; Kavala/GR

Purpose: Blunt abdominal trauma is a diagnostic challenge to the emergency radiology. The aim of the study is to determine FAST (focused assessment with sonography for trauma) as screening method in trauma patients with blunt abdominal injuries.

Material and Methods: From March 2008 to April 2009, we examined in our department with ultrasonagraphy (FAST) according to protocol 756 hemodynamically stable trauma patients with suspected blunt abdominal injuries. In most of these cases, a CT scan was necessary to be performed.

Results: Ultrasonography examination was positive in 72 patients. The results of FAST were compared with findings of CT scan, diagnostic peritoneal lavage, laparotomy and clinical course when the FAST was positive or followed by a period of clinical observation when the FAST was negative.

Conclusion: The FAST examination is a routine component of the initial work-up of trauma patients with high sensitivity to detect free fluid which would lay a suspicion for a parenchyma lesion. We must remember that a negative ultrasonography does not exclude an abdominal injury. In this case, another imaging procedure such as CT should be performed.

Other / Radiologic-Pathologic Correlation

SE-086

Optimization of b value in diffusion MRI for detection and characterization of abdominal benign and malignant lesions

Z. Koc, G. Erbay, S. Ulusan, B. Kaya, G. Seydaoglu; Adana/TR

Purpose: To determine the optimal b value in diffusion-weighted imaging (DWI) for detection and differentiation of benign and malignant abdominal lesions.

Material and Methods: Routine abdomen MRI and single shot echo planar DWI were prospectively performed using seven b values (50, 200, 400, 500, 600, 800, 1000 s/mm^2). 66 lesions in 58 patients who had pathologically proven diagnosis of the malignant or benign diseases obtained after MRI examinations were included. The image quality was analyzed on a five-point scale and by measurement of the signal-to-noise ratio (SNR). The lesion detectability was analyzed by measurement of the contrast-to-noise ratio (CNR). The lesions were analyzed for benignity/malignity on a 5 point scale, and by measurement of the apparent diffusion coefficient (ADC) values and lesion ADC/normal parenchyma ADC.

Results: Significant differences were found in visual scores between different b values ($p<0.01$). Lower b values correlated with better DW image quality and lesion detectability. The SNR and CNR with b values of 50 and 200 s/mm^2 were significantly high from that with b400 and higher b values. Differentiation of malignant from benign abdominal lesions using visual scoring was found successful with 600 and higher b values. The mean ADC values of malignant lesions inversely correlated with b values. The mean ADC values with a b value of 200 s/mm^2 and ADC ratio for b200 and ADC with all b values of malignant lesions were significantly lower than those of benign lesions on DWI ($p<0.05$).

Conclusion: Image quality and lesion detectability are better with low b values around 50 and 200 s/mm^2. The lesion ADC/normal parenchyma ADC are more accurate for differentiation of malignant and benign abdominal lesions.

SE-087

Abdominal lesions in post-mortem non-enhanced CT-scan: correlations with forensic autopsy

P. Charlier[1], R. Carlier[1], F. Roffi[1], J. Ezra[1], F. Duchat[2], G. Lorin De La Grandmaison[1], I. Huynh-Charlier[2]; [1]Garches/FR, [2]Paris/FR

Purpose: To investigate the interest of post-mortem non-enhanced CT for abdominal damages in a forensic context of suspect death.

Material and Methods: 30 cadavers have been submitted to a body CT-scan without injection of contrast material. CT exams were reviewed by two independent radiologists and radiological findings were compared with forensic autopsy data.

Results: False negative CT findings included small contusions, vascular thromboses, acute infarcts foci, and non-radioopaque foreign bodies. False positive CT findings included physiological post-mortem transudates misdiagnosed with intra-abdominal bleedings and putrefaction gas misdiagnosed with gas embolism, aeroporty, aerobily, digestive parietal pneumatosis. Incidentalomas without any role in death process were also reported. CT could diagnose solid organ fractures, digestive perforations, hematomas and massive hemorrhages, metallic foreign bodies, advanced tumors, aortic dissections (when the flap was calcified). CT was helpful to guide autopsy and to show knife and ballistic trajectories. CT showed postoperative scars (on vascular map, biliary tree, digestive tract or solid organs) which were anatomical arguments during identification process. CT images constituted an useful numerical memory of the cadaver for cross-examination.

Conclusion: The radiologist should be familiar with the normal abdominal post-mortem features to avoid misdiagnoses and detect informative lesions which can help and guide the forensic practitioner. This study shows the interest of a radiological examination of cadavers by CT (even without any injection of contrast material) before forensic autopsy.

DOI: 10.1007/s00330-010-1777-8

多段階発癌・早期肝細胞癌の画像診断と病理・病態
― a.CT・動注CT ―

上田和彦* 柳沢 新* 山崎幸恵* 渡辺智治*
山田 哲* 松下 剛* 平瀬雄一* 黒住明子*
黒住昌弘* 藤永康成* 角谷眞澄*

肝細胞癌の母体となる結節のCT診断では，背景にある血流動態を知るとよい．

Key Word 肝細胞癌，CT，血管造影

はじめに

硬変肝には種々の肝細胞性結節が出現する．そのうちの一部から肝細胞癌(hepatocellular carcinoma, HCC)が発生する．この肝細胞癌の母体になりうる結節の拾い上げと，それらの結節から生まれる癌の察知が画像診断の役割である．本稿では，本疾患の動注CTの特徴とその背景にある病理・病態をまとめ，日常用いるCT診断における留意点を述べる．

1 肝細胞癌の母体となる結節とその癌化の組織学的血管支配

肝細胞癌の母体となる結節およびその癌化のプロセスと，動脈と門脈で個別に計測した組織学的血管密度との相関は，hepatocarcinogenesisを画像で解析する際のバックボーンとして利用されてきた．その概要は以下のとおりである[1]．

1) 動脈，門脈の両方が背景の肝硬変と同等の結節は，通常型腺腫様過形成(ordinary adenomatous hyperplasia, OAH)［low grade dysplastic nodule(low-DN)に相当］であった．

2) 動脈，門脈の両方が肝硬変に比し減少を示す結節は，通常型腺腫様過形成あるいは異型腺腫様過形成(atypical adenomatous hyperplasia, AAH)［high grade dysplastic nodule(high-DN)に相当］のいずれかであった．

3) 動脈が同等で，門脈が減少している結節は，主として異型腺腫様過形成であった．

4) 動脈が増加，門脈が減少する結節は肝細胞癌であり，大半(83.3%)の肝細胞癌結節内に門脈は見られなかった．

5) 結節内に出現するすべての動脈面積に対する異常動脈面積の占める割合を検討すると，通常型腺腫様過形成(17.5%)，異型腺腫様過形成(52.5%)，肝細胞癌(92.0%)の順に増加していた．

これらの結果より導き出された概念を図1に示す．画像診断を行う際は，この概念を基に個々の画像を解析する．

* Ueda K., Yanagisawa S., Yamazaki S., Watanabe T., Yamada S., Matsushita T., Hirase Y., Kurozumi A., Kurozumi M., Fujinaga Y., Kadoya M. 信州大学医学部画像医学講座

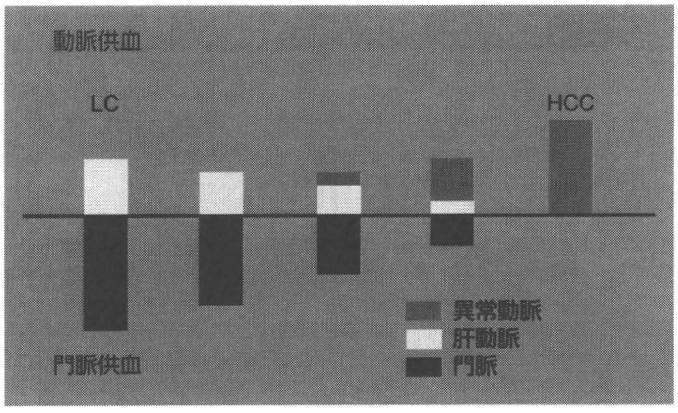

図1　肝細胞癌の母体となる結節の癌化と組織学的血管支配

2 組織学的悪性度と，動注CTで観察される生体内血管支配

組織学的悪性度と組織学的血管支配の関係が生体内でも当てはまるか検討された[2]．その概要は以下のとおりである．

1) 結節の経動脈性門脈造影下CT (CTAP) 上の濃度を，

a. 背景と等吸収，
b. 背景よりわずかに低吸収，
c. 結節の一部が背景に比し明瞭な低吸収，
d. 結節の全体が背景に比し明瞭な低吸収，

の4型に分類すると，low-DNの77%がa，high-DNの68%がaかb，w-HCC（高分化型肝細胞癌）の54%がc，29%がd，mp-HCC（中低分化型肝細胞癌）の100%がdを示した．

2) 結節の肝動脈造影下CT (CTHA) 上の濃度を，

I. 背景と等吸収，
II. 背景に比し低吸収，
III. 背景に比し一部が高吸収，
IV. 背景に比し全体が高吸収，

の4型に分類すると，

low-DNの69%がI，
high-DNの68%がIかII，
w-HCCの53%がIII，40%がIV，
mp-HCCの100%がIV，

を示した．

これらの結果から結節の組織学的悪性度が増加するに従い，CTAPではaからdへ，CTHAではIからIVへと移行することがわかった．

3) CTAP，CTHAの両方が施行された結節では，

low-DNの58%がa-I，27%がa-II，
high-DNの37%がa-II，16%がa-I，16%がa-II，11%がc-II，11%がc-III，
w-HCCの47%がc-III，33%がd-IV，
mp-HCCの100%がd-IV，

を示した．

3 癌の母体となる結節の組織学的特徴

複数の組織学的所見の有無と，経過による悪性度の関連が検討されている．それによれば，癌の母体となる可能性が高くなる結節には，核密度の上昇，明細胞化，small cell dysplasia，脂肪化が見られるとされている[3]．

4 動注CTで観察される生体内血管支配と経過から見た癌化の確率

結節の真の悪性度を知るには結節の経過を見るとよい．多数例を画像所見を基に9群に分類し，各群に属する結節が，1年で結節全体が癌化する確率，1年後には癌化しないが2年後には結節全体が癌化する確率，2年経ても結節全体が癌化しない確率を調べた[4] (図2)．

1) 1年後に結節全体が肝細胞癌に変化する確率が高い結節は，動脈供血が増加かつ門脈供血が欠損する領域を内包する結節である．

2) 2年経っても肝細胞癌に変化する可能性が低い結節は次のとおりである．

i. 門脈供血と動脈供血がいずれも背景と差がない結節，
ii. 門脈供血は差がないが，動脈供血が減少している結節，

図2　動注CTと癌化への経過
各群の数字は，上段：結節数，中段：1年後に癌化した結節の百分率，下段：2年後に癌化した結節の百分率．

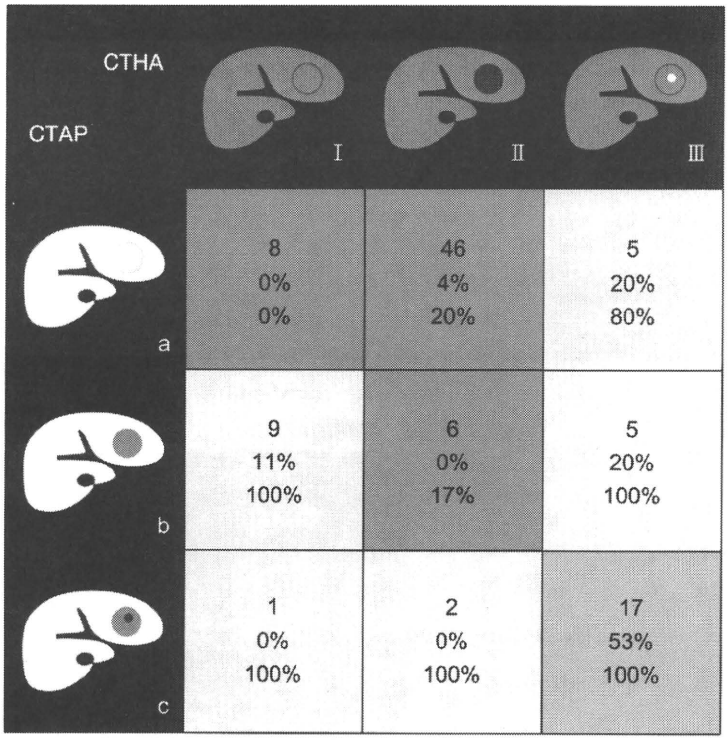

iii. 門脈供血と動脈供血がいずれも減少している結節，

3) その他の結節は1年後には肝細胞癌になっていないが，2年後には肝細胞癌に変化している可能性が高い結節である．

4) この結果で興味深いのはa-Iとb-Iの群の違いである．両者は門脈供血が異なるのみで，動脈供血は同じであるにもかかわらず，2年後の経過は全く異なる．**図1**に示した組織計測による検討を基に考えると，一見同じである両者の動脈供血はその内容が異なるのではないかと推測できる．すなわち，a-Iの結節の動脈供血は正常肝動脈由来であるのに対し，b-Iの結節は異常動脈由来である可能性が高い．前者は**図1**のいちばん左のバーに当たり，後者は右から2番目のバーに当たる．ちなみにa-IIの結節は**図1**の左から2あるいは3番目のバーに当たる．この経過と動注CTの対比の結果は，**図1**の妥当性を経過の点でも支持するものと言える．

5) 本検討により結節の成長（悪化）と供血の仕組みが明らかになり，動注CTを用い動脈供血と門脈供血を個々に評価することで結節の予後推定が容易になった．

5 動注CTで得た知見のCTへの外挿

硬変肝に発生する結節のCT診断の概要は以下の2点である．

1）拾い上げ（図3）

いずれかの時相で癌の母体となる結節を拾う．背景肝と濃度差が生ずるなら，いずれの時相でも低濃度を呈する．その頻度が高い単純CTと造影CT晩期を重点的に観察する．

2）発癌の察知（図4～6）

癌の母体となる結節を拾い上げたら，その結節の内部に早期濃染の有無を確かめる．

おわりに

肝細胞癌の母体となる結節および早期肝細胞癌における，動注CTおよびCT診断は，背景にある病理・病態を理解すれば容易である．CTでは単純および造影後期相を重点的に観察して，結節の拾い上げに留意するのがポイントである．

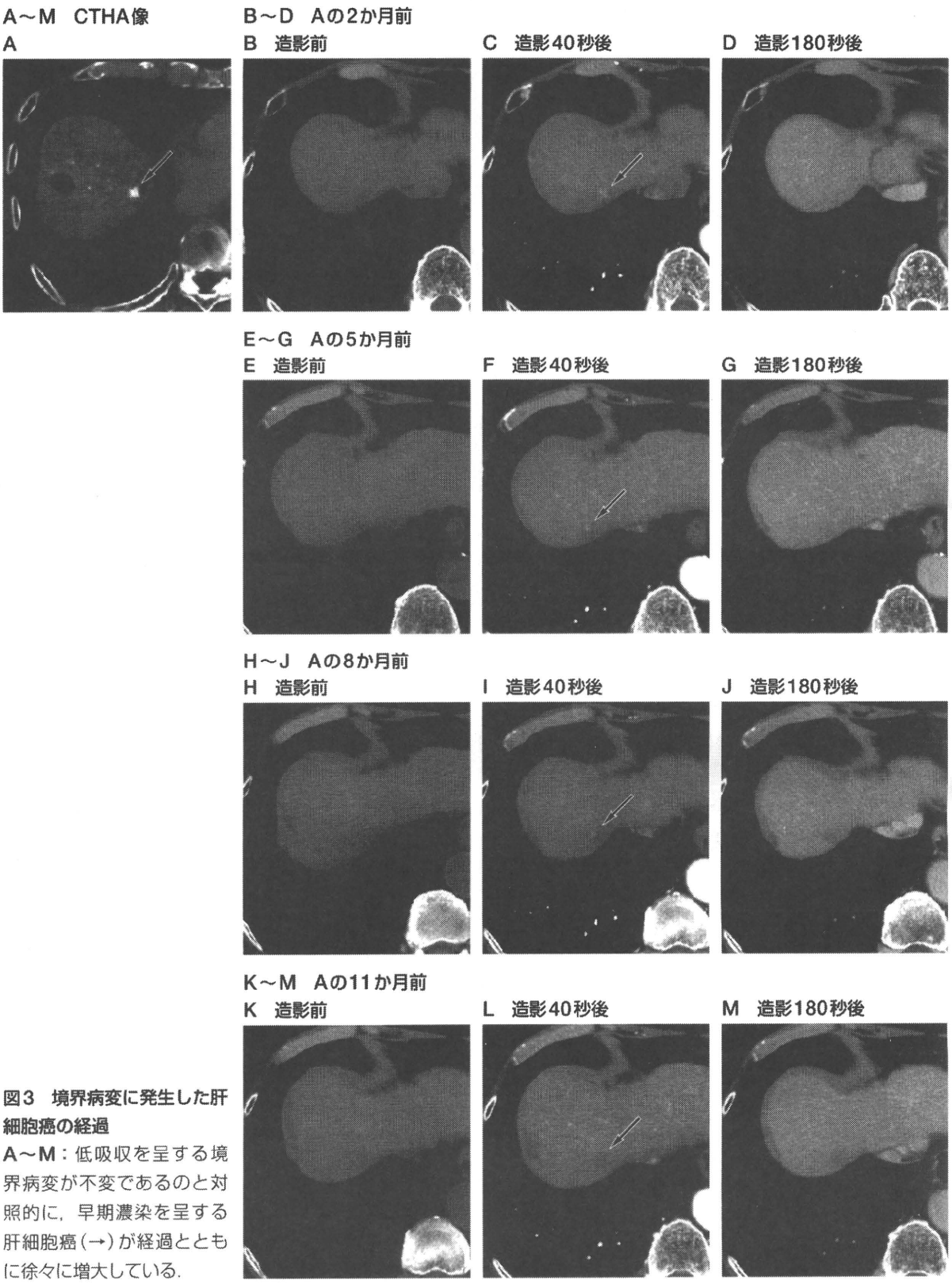

図3　境界病変に発生した肝細胞癌の経過

A～M：低吸収を呈する境界病変が不変であるのと対照的に，早期濃染を呈する肝細胞癌(→)が経過とともに徐々に増大している．

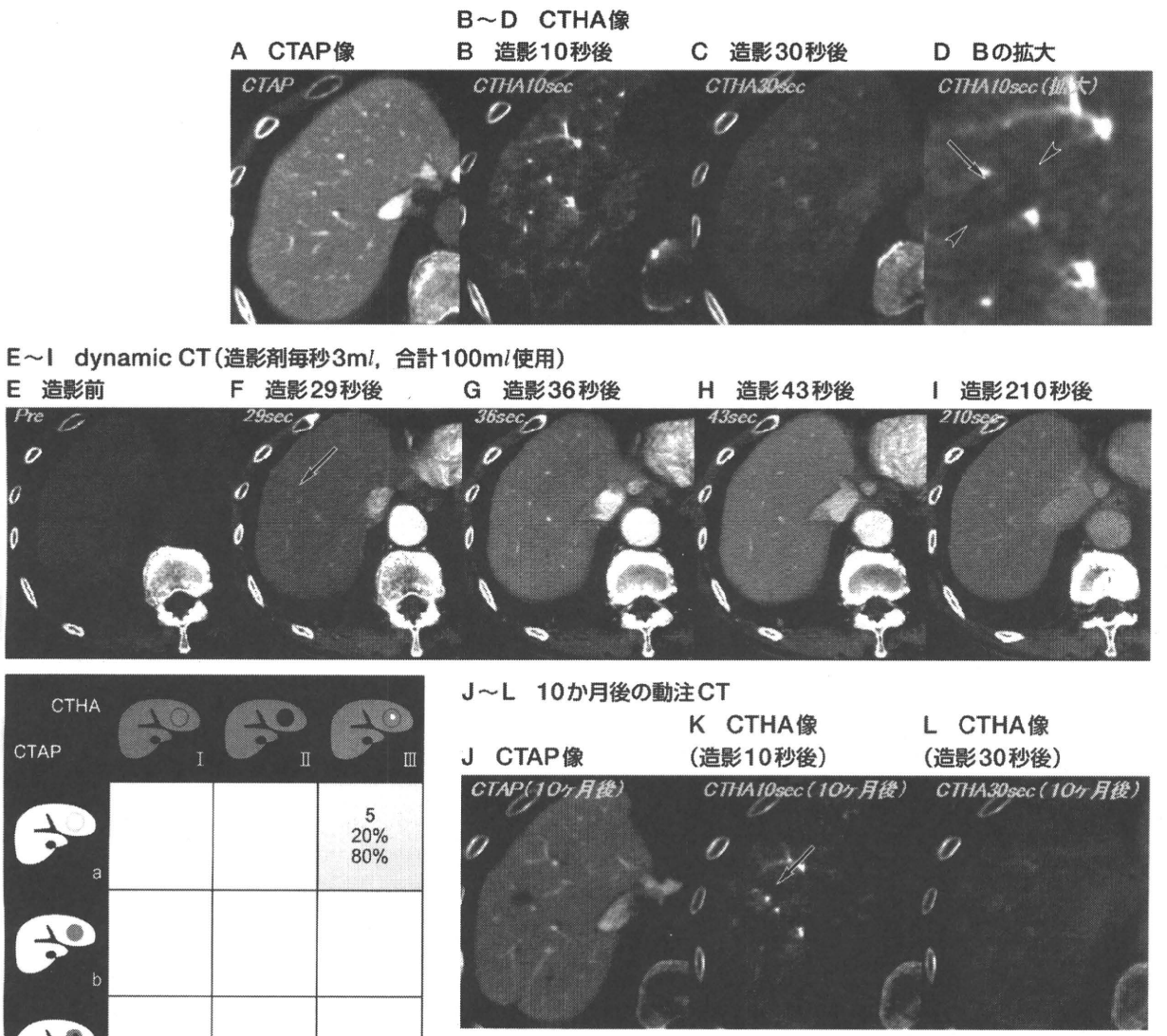

図4　境界病変に発生した肝細胞癌の経過

A～D：CTAP(**A**)で結節全体が背景肝と等濃度，CTHA(**B～D**)にて境界病変(**D**；►)が背景より低濃度，癌(**D**；→)が高濃度を呈し，表の上段右端(a-III)の結節に相当する．

E～I：他のどの時相においても，境界病変は背景肝と等濃度を呈し視認できないのに対し，造影後29秒後にのみ癌は高濃度を示した(**F**；→)．

J～L：10か月後で癌が増大し，結節の大部分を置換している(**K**；→)．

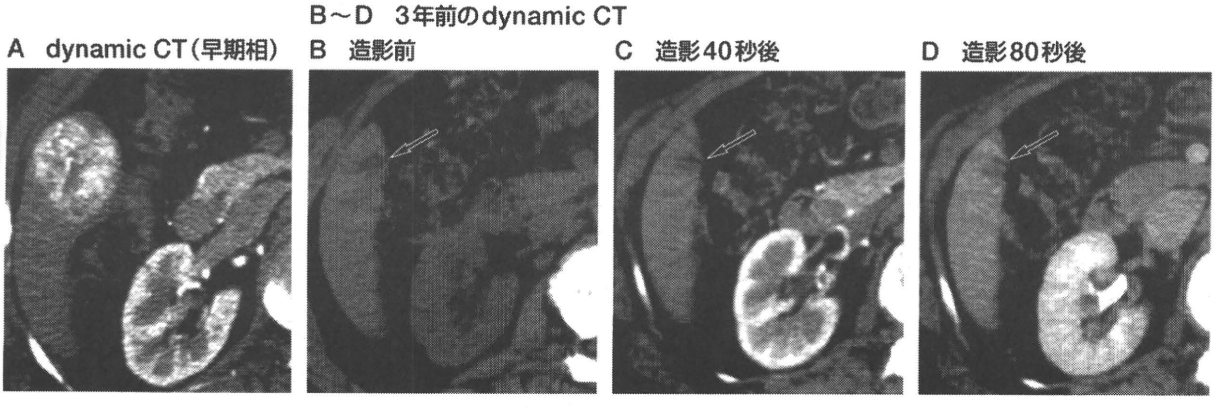

図5　境界病変から発生した肝細胞癌

B～D：どの時相でも低濃度を呈している(→)．本図には示さないが2年前のMRIでは遡及的に見ても同定できなかった．